

Reactions of the spiro monoanion $[\{(Me_2N)Sb(\mu\text{-NCy})_2\}_2Sb]^-$ with alcohols and thiols (REH; E = O or S); syntheses of *nido*- $[Sb_3(\mu\text{-NCy})_3(\mu_3\text{-NCy})(ER)_2]$ anions and the unique antimony(III) imido cubane $[(2\text{-NC}_5\text{H}_4\text{O})Sb(\mu_3\text{-NCy})]_4$ (Cy = cyclohexyl)

Alan Bashall,^a Michael A. Beswick,^b Neil Feeder,^b Alexander D. Hopkins,^b Sara J. Kidd,^b Mary McPartlin,^a Paul R. Raithby^b and Dominic S. Wright^{*b}

^a School of Chemistry, University of North London, London, UK N7 8DB

^b Chemistry Department, University of Cambridge, Lensfield Road, Cambridge, UK CB2 1EW.
Fax: 01223 336362; E-mail dsw1000@cus.cam.ac.uk

Received 17th February 2000, Accepted 25th April 2000

Published on the Web 24th May 2000

Reactions of $Sb(NMe_2)_3$ with a mixture of $CyNH_2$ and Pr^i_2NM (1 : 1 : 1 equivalents) afforded a simple route to $M[\{(Me_2N)Sb(\mu\text{-NCy})_2\}_2Sb]$ (M = Li **1**·Li or Na **1**·Na), containing the spiro anion $[\{(Me_2N)Sb(\mu\text{-NCy})_2\}_2Sb]^-$ **1**. The reactions of **1**·Li with $tBuOH$ / $tBuOK$ and with $2\text{-HS}\{1\text{-Me(imid)}\}$ (imid = imidazole) (2 equivalents) gave $[K\cdot\eta^6\text{-C}_6\text{H}_5\text{Me}][Sb_3(\mu\text{-NCy})_3(\mu_3\text{-NCy})(O^tBu)_2]$ **2** and $Li[Sb_3(\mu\text{-NCy})_3(\mu_3\text{-NCy})(S\{2\text{-Me(imid)}\})_2]$ **3**, respectively, in which the spiro structure of the precursor rearranges into a *nido* framework. Reaction of **1**·Li with $HOC_5H_4N\text{-}2$ led to disintegration of the Sb_3N_6 anion core and formation of the unique antimony(III) imido cubane $[(2\text{-NC}_5\text{H}_4\text{O})Sb(\mu_3\text{-NCy})]_4$ **4**. The crystal structures of the new complexes **1**·Na, **3** and **4** were determined.

Ligand systems based on imido Group 15 element frameworks can readily be accessed by the step-wise reactions of dimethyl-amido Group 15 reagents $E(NMe_2)_3$ (E = As, Sb or Bi) with primary amido alkali metal complexes.¹ Ligands such as the tripodal trianions $[E(NR)_3]^{3-}$ and the tetradentate dianions $[E_2(NR)_4]^{2-}$ have an extensive co-ordination chemistry,² the reactions of their alkali metal complexes with a range of main group and transition metal sources giving heterometallic cages in which the imido Group 15 frameworks are preserved. Recent interests in these ligands have focused on their potential ability to modify and control the bonding and magnetic interactions within supported metal cores,³ and the use of phosphinidene analogues of the imido complexes as single-source precursors for the deposition of metallic alloys.⁴

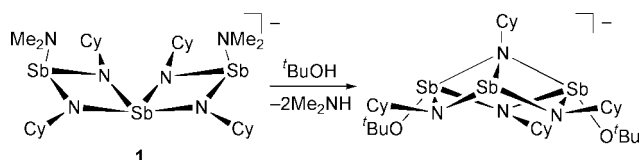
A further interest of ours concerns the selective functionalisation of existing ligand arrangements, allowing potential ligand-selective behaviour towards metal ions. In a recent communication we showed that the reaction of the antimony(III) anion $[\{(Me_2N)Sb(\mu\text{-NCy})_2\}_2Sb]^-$ **1** (Cy = cyclohexyl) with $tBuOH$ (2 equivalents) results in rearrangement of the spiro structure into a *nido* framework, $[Sb_3(\mu\text{-NCy})_3(\mu_3\text{-NCy})(O^tBu)_2]^-$ (Scheme 1).⁵ This observation is in contrast to the

arrangement in which there is a net increase in the co-ordination numbers of two of the antimony centres.

We report here a new, convenient synthesis of the spiro-monoanion $[\{(Me_2N)Sb(\mu\text{-NCy})_2\}_2Sb]^-$ **1** from the one-pot reaction of $Sb(NMe_2)_3$ with $CyNH_2$ and Pr^i_2NM (M = Li or Na). This new approach has facilitated more in-depth investigations of the reactions of this monoanion with various organic acids. In addition to $[K\cdot\eta^6\text{-C}_6\text{H}_5\text{Me}][Sb_3(\mu\text{-NCy})_3(\mu_3\text{-NCy})(O^tBu)_2]$ **2**,⁵ the syntheses and structures of the new spiro-monoanion complex $Na[\{(Me_2N)Sb(\mu\text{-NCy})_2\}_2Sb]$ **1**·Na, the *nido*-monoanion complex $Li[Sb_3(\mu\text{-NCy})_3(\mu_3\text{-NCy})(2\text{-S}\{1\text{-Me(imid)}\})_2]$ **3** (imid = imidazole), and the unusual antimony(III) imido cubane $[(2\text{-NC}_5\text{H}_4\text{O})Sb(\mu_3\text{-NCy})]_4\cdot 0.5C_6H_5Me$ **4** (all derived from reactions of the parent monoanion with organic alcohols and thiols) are reported.

Discussion

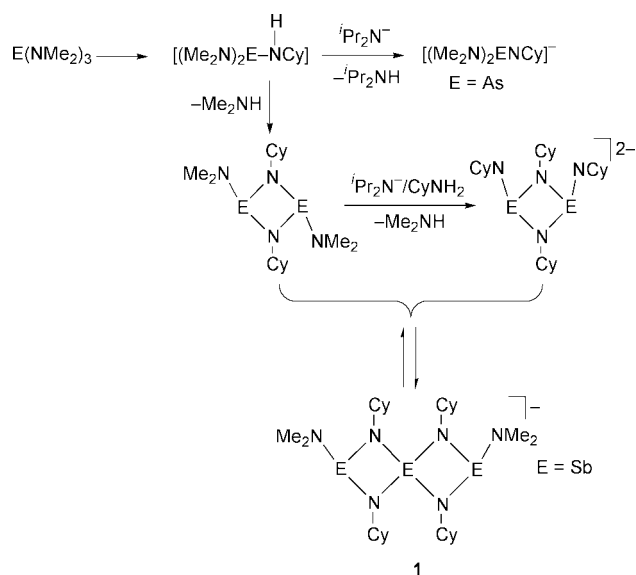
We had shown in earlier work that the spiro-monoanion $[\{(Me_2N)Sb(\mu\text{-NCy})_2\}_2Sb]^-$ can be obtained as its Li^+ salt in relatively low yield (32%) from the *in situ* reaction of $Li[Sb(NHCy)_4]$ with $Sb(NMe_2)_3$ (1 : 2 equivalents).⁶ The same monoanion framework is also accessible *via* the one-pot reactions of $CyNHM$ (M = K or Rb), $CyNH_2$ and $Sb(NMe_2)_3$, although in this case in the form of the substituted derivative $[(CyNH)Sb(\mu\text{-NCy})_2\}_2Sb]^-$.⁷ For some time we had investigated various potentially higher yielding pathways to the parent monoanion containing terminal Me_2N groups, which would facilitate more extensive functionalisation of the imido antimony(III) core with other donor groups. In related work we observed recently that the reaction of $As(NMe_2)_3$ with $CyNHK$ in the presence of Pr^i_2NK gave smooth formation of the $[(Me_2N)_2\text{-}As(NCy)]^-$ anion.⁸ The analogous reactions of $Sb(NMe_2)_3$ with $CyNH_2$ and Pr^i_2NM (M = Li or Na) were undertaken with a view to obtaining related antimony(III) complexes containing the $[(Me_2N)_2Sb(NCy)]^-$ anion. However, surprisingly the spiro-monoanion $[\{(Me_2N)Sb(\mu\text{-NCy})_2\}_2Sb]^-$ **1** is obtained from these reactions (in the form of the salts **1**·Li and **1**·Na



Scheme 1

reaction with $CyNH_2$ which results in simple replacement of the Me_2N groups and in retention of the spiro core of the ligand, in the product $[\{(CyNH)Sb(\mu\text{-NCy})_2\}_2Sb]^-$.^{2a} The difference between the outcomes of the reactions involving $tBuOH$ and $CyNH_2$ was attributed to the greater electronegativity of O. This factor, it was reasoned, would lead to an increase in the Lewis acidity of the metal atoms, resulting in the *nido* cage

respectively). The key difference between the results of the reactions involving $\text{As}(\text{NMe}_2)_3$ and $\text{Sb}(\text{NMe}_2)_3$ appears to lie in the competition between inter- and intramolecular deprotonation of the intermediates $[(\text{Me}_2\text{N})_2\text{E}(\text{NHCy})]$ ($\text{E} = \text{As}$ or Sb), as depicted in the proposed mechanism shown in Scheme 2.



Scheme 2

In the case of the arsenic(III) intermediate $[(\text{Me}_2\text{N})_2\text{As}(\text{NHCy})]$ intermolecular deprotonation by Pr_2NK (giving Pr_2NH) occurs faster than intramolecular deprotonation (elimination of Me_2NH). However, the presence of more polar $\text{Sb}-\text{N}$ bonds in the antimony analogue results in the formation of the dimer $[(\text{Me}_2\text{N})\text{Sb}(\mu\text{-NCy})_2]$, via an intramolecular pathway. Various examples of dimers of this type have structurally been characterised previously.⁹ Several pathways to the monoanion framework $[\{(\text{Me}_2\text{N})\text{Sb}(\mu\text{-NCy})_2\}_2\text{Sb}]^-$ **1** can be envisaged. The most reasonable involves equilibration of the dianion $[\text{Sb}_2(\text{NCy})_4]^{2-}$ with the dimer $[(\text{Me}_2\text{N})\text{Sb}(\mu\text{-NCy})_2]$, the former resulting from further reaction of the dimer with CyNHM .

The significance of this new approach to the spiro- $[\{(\text{Me}_2\text{N})\text{Sb}(\mu\text{-NCy})_2\}_2\text{Sb}]^-$ framework is that it furnishes the required starting point for the investigation of the reactions and functionalisation of this key ligand; the principal starting material $\text{Li}[\{(\text{Me}_2\text{N})\text{Sb}(\mu\text{-NCy})_2\}_2\text{Sb}]$ **1**·Li being isolated in crystalline form in 88% yield. A large range of reactions of **1**·Li with various organic acids (primary amines, phosphines, alkoxides and thiols, including those possessing donor functionality on their organic substituents) were undertaken. However, in most cases no pure materials could be isolated or (as in the case of phosphines) the complexes formed were too unstable. Most successful were reactions involving the more acidic alcohols or thiols. Varying degrees of fragmentation of the spiro- $[\{(\text{Me}_2\text{N})\text{Sb}(\mu\text{-NCy})_2\}_2\text{Sb}]^-$ anion **1** are exhibited in these reactions, which depend largely on the acidity of alcohol or thiol used.

The selective reaction of the terminal Me_2N groups of the spiro- $[\{(\text{Me}_2\text{N})\text{Sb}(\mu\text{-NCy})_2\}_2\text{Sb}]^-$ framework of **1** was observed in our previously communicated synthesis of $[\text{K} \cdot \eta^6\text{-C}_6\text{H}_5\text{Me}][\text{Sb}_3(\mu\text{-NCy})_3(\mu_3\text{-NCy})(\text{O}^t\text{Bu})_2]$ **2**.⁵ This is generated from the reaction of $\text{Li}[\{(\text{Me}_2\text{N})\text{Sb}(\mu\text{-NCy})_2\}_2\text{Sb}]$ **1**·Li with $^t\text{BuOK}$ (1 equivalent) followed by reaction of the intermediate $\text{K}[\{(\text{Me}_2\text{N})\text{Sb}(\mu\text{-NCy})_2\}_2\text{Sb}]$ **1**·K with $^t\text{BuOH}$ (2 equivalents). The result of the second step is the rearrangement of the spiro framework of the anion **1** into a *nido* anion, $[\text{Sb}_3(\mu\text{-NCy})_3(\mu_3\text{-NCy})(\text{O}^t\text{Bu})_2]^-$ (see Scheme 1). As is discussed in the introduction, it had been assumed that the primary reason for this unusual rearrangement is the increased electronegativity of

the oxygen substituent. However, the same rearrangement is also observed in the reaction of **1**·Li with 1-methyl-2-sulfanylimidazole $[2\text{-HS}\{1\text{-Me}(\text{imid})\}]$, giving $\text{Li}[\text{Sb}_3(\mu\text{-NCy})_3(\mu_3\text{-NCy})(2\text{-S}\{1\text{-Me}(\text{imid})\})_2]$ **3** in which the Me_2N groups are replaced by $2\text{-S}\{1\text{-Me}(\text{imid})\}$ groups. Although the imidazole substituent will have a significant electron-withdrawing influence, it seems unlikely that the effect of the electronegativity of the substituents alone can explain why this rearrangement occurs in the cases of **2** and **3**, and yet is not observed in the reaction of anion **1** with CyNH_2 ^{2a} [the electronegativity of S (2.58 on the Pauling scale) being similar to that of N (2.55) and considerably lower than that of O (3.44)¹⁰]. It is possible that the *nido* and spiro arrangements are close in energy and that further factors such as the steric demands of the substituents, the attainment of optimum co-ordination of the alkali metal cations involved and (relevant to the later structural characterisation of the toluene solvate $3 \cdot 0.5\text{C}_6\text{H}_5\text{Me}$) the promotion of intermolecular interactions can tip the balance between these isomeric alternatives.

More extensive fragmentation of the spiro-framework of anion **1** is observed in its reaction with $2\text{-NC}_5\text{H}_4\text{OH}$ (1:2 equivalents, respectively), giving the cubane $[(2\text{-NC}_5\text{H}_4\text{O})\text{Sb}(\mu\text{-NCy})_4]$ **4** (isolated as the toluene solvate, $4 \cdot 0.5\text{C}_6\text{H}_5\text{Me}$). The formation of **4** provides further support for the suggestion that the anion $[\{(\text{Me}_2\text{N})\text{Sb}(\mu\text{-NCy})_2\}_2\text{Sb}]^-$ **1** is in equilibrium with the dimer $[(\text{Me}_2\text{N})\text{Sb}(\mu\text{-NCy})_2]$ and the dianion $[\text{Sb}_2(\text{NCy})_4]^{2-}$ in solution, as is implied by the isolation of **1**·Li (in high yield) from the reaction of $\text{Sb}(\text{NMe}_2)_3$ with CyNH_2 and Pr_2NLi (shown in Scheme 2). In addition to the high solubility of **4** in organic solvents, the low yield of the complex (10%, on the basis of Sb supplied) can also be attributed to the fact that only a fraction of the monoanion **1** is available for reaction (*i.e.*, the dimer). It is interesting in this regard that **4** is accessible in increased yield from the reaction of $[(\text{Me}_2\text{N})\text{Sb}(\mu\text{-NCy})_2]$ with $2\text{-NC}_5\text{H}_4\text{OH}$ (1:2 equivalents, respectively; 31%). The greater fragmentation of the core of **1**·Li observed in **4** appears to be broadly consistent with the greater acidity of $2\text{-NC}_5\text{H}_4\text{OH}$ (*cf.* the formation of the *nido*-arrangement of **2** from the reaction with $^t\text{BuOH}$). However, the greater extent of reaction which we have observed in the formation of the known complex $[\text{Sb}(2\text{-SC}_5\text{H}_4\text{N})_4]$ **5**¹¹ from the reaction of **1**·Li with 2-sulfanylpipridine ($2\text{-HSC}_5\text{H}_4\text{N}$) (1:2 equivalents, respectively) does not appear to fit this trend (*cf.* the formation of the *nido*-arrangement of **4** from the reaction with $2\text{-HS}\{1\text{-Me}(\text{imid})\}$). The steric demands and co-ordination characteristics of the organic substituents may also play a role in influencing the species formed in these reactions.

Prior to their structural characterisations by X-ray crystallography, the basic identities of the new complexes **1**·Na, **3** and **4** were determined using a combination of IR and ^1H NMR spectroscopy as well as by elemental analyses (C, H, N). These data show that solvation by toluene is retained even in vacuum-dried samples of **3** and **4**. Tables 1, 2 and 3 give key bond lengths and angles for **1**·Na, $3 \cdot 0.5\text{C}_6\text{H}_5\text{Me}$ and $4 \cdot 0.5\text{C}_6\text{H}_5\text{Me}$ respectively. Details of the low-temperature structure of complex **2** (having a *nido* structure related to that of **3**) have been communicated previously and no further discussion will be provided here, except by way of comparison.⁵

The low-temperature structure of $\text{Na}[\{(\text{Me}_2\text{N})\text{Sb}(\mu\text{-NCy})_2\}_2\text{Sb}]$ **1**·Na (Fig. 1) shows that the complex is an ion-paired species, composed of a $[\{(\text{Me}_2\text{N})\text{Sb}(\mu\text{-NCy})_2\}_2\text{Sb}]^-$ monoanion which co-ordinates a Na^+ cation. The co-ordination mode is identical to that occurring in the Li^+ analogue $\text{Li}[\{(\text{Me}_2\text{N})\text{Sb}(\mu\text{-NCy})_2\}_2\text{Sb}]$ **1**·Li,⁶ involving bonding of both of the pendant Me_2N groups [$\text{Na}(1)-\text{N}(5,6)$ mean 2.43 Å] and the two equatorial NCy groups of the 10e pseudo trigonal bipyramidal antimony centre [$\text{Na}(1)-\text{N}(1,4)$ mean 2.46 Å] to the metal cation. This structural design is also similar to that occurring in the related heavier alkali metal complexes $[\text{M} \cdot 2\text{thf}][\{(\text{CyNH})\text{Sb}(\mu\text{-NCy})_2\}_2\text{Sb}]$ ($\text{M} = \text{K}$ or Rb),⁷ although here the

Table 1 Key bond lengths (Å) and angles (°) for Na[$\{(\text{Me}_2\text{N})\text{Sb}(\mu\text{-NCy})_2\}_2\text{Sb}\}$ **1**·Na

Sb(1)–N(2)	1.98(1)	Sb(3)–N(3)	1.97(1)
Sb(1)–N(4)	2.04(1)	Sb(3)–N(5)	2.13(2)
Sb(1)–N(6)	2.14(1)	Na(1)–N(1)	2.45(2)
Sb(2)–N(1)	2.10(1)	Na(1)–N(4)	2.48(1)
Sb(2)–N(2)	2.23(1)	Na(1)–N(5)	2.45(2)
Sb(2)–N(3)	2.23(1)	Na(1)–N(6)	2.41(2)
Sb(2)–N(4)	2.11(1)	Na(1A)···C(H)	3.06
Sb(3)–N(1)	2.04(1)		
N(2)–Sb(1)–N(4)	81.3(5)	N(4)–Sb(2)–N(3)	83.7(5)
N(2)–Sb(1)–N(6)	96.7(5)	N(1)–Sb(3)–N(3)	79.9(5)
N(4)–Sb(1)–N(6)	92.1(5)	N(1)–Sb(3)–N(5)	92.6(6)
N(1)–Sb(2)–N(2)	87.3(4)	N(3)–Sb(3)–N(5)	95.7(6)
N(1)–Sb(2)–N(3)	72.8(5)	N(5)–Na(1)–N(6)	165.9(6)
N(1)–Sb(2)–N(4)	97.6(5)	N(1)–Na(1)–N(4)	80.0(5)
N(2)–Sb(2)–N(3)	148.1(5)	N(1,4)–Na(1)–N(5,6)	76.0(5)
N(4)–Sb(2)–N(2)	74.2(5)		

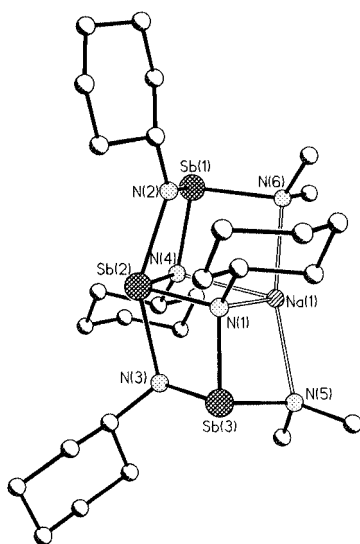


Fig. 1 Structure of molecules of Na[$\{(\text{Me}_2\text{N})\text{Sb}(\mu\text{-NCy})_2\}_2\text{Sb}\}$ **1**·Na with H-atoms omitted for clarity.

cations are additionally co-ordinated by two thf ligands (resulting in highly distorted octahedral metal geometries).

Apart from providing unequivocal proof of the success of the new synthetic route to the monoanion framework **1**, the significance of the structural characterisation of **1**·Na is that it completes the missing link in the related series of monoanion complexes containing Li, K and Rb which have been characterised previously.^{6,7} Some general comments can be made in this regard. First, the pattern of long, medium and short Sb–N bond lengths within the spiro Sb_3N_6 core of **1**·Na is exactly the same as that observed in the structures of $\text{Li}\{[(\text{Me}_2\text{N})\text{Sb}(\mu\text{-NCy})_2]_2\text{Sb}\}$ **1**·Li and $[\text{M} \cdot 2\text{thf}][\{(\text{CyNH})\text{Sb}(\mu\text{-NCy})_2\}_2\text{Sb}]$ ($\text{M} = \text{K}$ or Rb), despite the differences in the ionic sizes and extents of Lewis base solvation of the alkali metal cations present. Like all these previously characterised complexes, the longest Sb–N bonds in the core of **1**·Na occur at the axial positions of the pseudo trigonal bipyramidal Sb atom [Sb(2)–N(2,3) mean 2.23(1) Å], with bonds of intermediate length being found at the equatorial positions [Sb(2)–N(1,4) mean 2.11(1) Å] and with the shortest bonds being made with the terminal, three-co-ordinate antimony centres [Sb(1,3)–N(1,2,3,4) mean 2.01 Å]. Secondly, as had been concluded previously from the solid-state structures of **1**·Li⁶ and $[\text{M} \cdot 2\text{thf}][\{(\text{CyNH})\text{Sb}(\mu\text{-NCy})_2\}_2\text{Sb}]$ ($\text{M} = \text{K}$ or Rb),⁷ the only significant difference between their cores is found in the equatorial N–Sb–N angles at the pseudo trigonal bipyramidal antimony centres of the anions. This angle roughly correlates with the ionic size of the alkali metal cation chelated by the

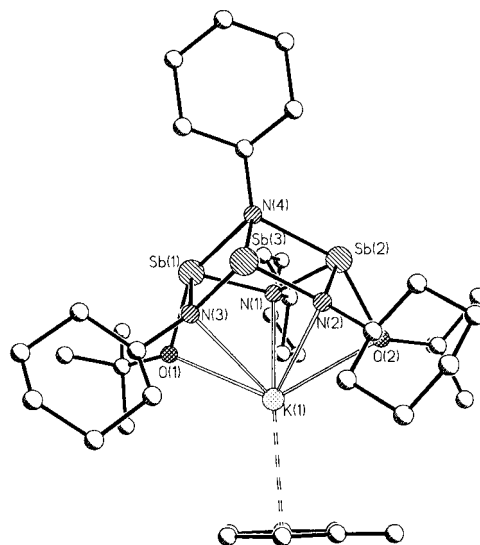


Fig. 2 Structure of molecules of $[\text{K} \cdot \eta^6\text{-C}_6\text{H}_5\text{Me}][\text{Sb}_3(\mu\text{-NCy})_3-(\mu_3\text{-NCy})(\text{O}'\text{Bu})_2]$ **2** with H atoms omitted for clarity.

equatorial NCy groups, and it is noteworthy that the corresponding angle in **1**·Na [N(1)–Sb(2)–N(4) 97.6(5)°] is entirely consistent with this view [*cf.* 92.5(2)° in **1**·Li and 100.5(3) and 101.0(4)° in $[\text{M} \cdot 2\text{thf}][\{(\text{CyNH})\text{Sb}(\mu\text{-NCy})_2\}_2\text{Sb}]$ for $\text{M} = \text{K}$ and Rb , respectively].

In the absence of further Lewis base solvation of the alkali metal cation of compound **2** (such as that found in the heavier alkali metal complexes $[\text{M} \cdot 2\text{thf}][\{(\text{CyNH})\text{Sb}(\mu\text{-NCy})_2\}_2\text{Sb}]$, the metal ion assumes a pseudo tetrahedral geometry which is similar to that occurring in **1**·Li.⁶ Presumably in order to make up for this relatively low co-ordination number, long-range intermolecular C(H)···Na contacts are found within the crystal lattice linking molecules of **1**·Na into a loose polymer. The distances involved (H···Na 3.06 Å) are significantly longer than those observed in a range of sodium complexes containing agostic C(H)···Na interactions, *i.e.* typically of the order of Na···C *ca.* 2.70–3.10 Å and Na···H *ca.* 2.30–2.60 Å in complexes in which there are strong intermolecular interactions.¹² In the previously characterised antimony(III) monoanion complex $[\text{K} \cdot 2\text{C}_6\text{H}_5\text{Me}][\{(\text{CyNH})\text{Sb}(\mu\text{-NCy})_2\}_2\text{Sb}]$ ^{2a} two toluene molecules are bound to the unsaturated K^+ ion by their CH_3 groups. A similar option is, we assume, not favourable for **1**·Na which (although prepared and crystallised from toluene–hexane solvent) has a more sterically congested core (*i.e.* as a result of the presence of far shorter Na–N bonds to the antimony(III) monoanion).

The cage structure of $[\text{K} \cdot \eta^6\text{-C}_6\text{H}_5\text{Me}][\text{Sb}_3(\mu\text{-NCy})_3(\mu_3\text{-NCy})(\text{O}'\text{Bu})_2]$ **2** (Fig. 2) is composed of a *nido*- $[\text{Sb}_3(\mu\text{-NCy})_3(\mu_3\text{-NCy})(\text{O}'\text{Bu})_2]^-$ anion which co-ordinates a K^+ cation at its open Sb_3N_3 face, using the three donor $\mu\text{-N}$ centres and the pendant O'Bu groups of the anion. In addition, the K^+ cation is further co-ordinated by an η^6 -toluene molecule, resulting in what can be viewed as a highly distorted six-co-ordinate geometry for the metal ion (if the η^6 -toluene ligand is assumed to occupy one co-ordination site). The structure of the anion of **2** is similar to that found for the neutral complex $[\text{Cl}_2\text{Sb}_2\text{Se}(\mu\text{-N}'\text{Bu})_3-(\mu_3\text{-N}'\text{Bu})]$.¹³

The low-temperature X-ray study of $\text{Li}[\text{Sb}_3(\mu\text{-NCy})_3-(\mu_3\text{-NCy})(2\text{-S}\{1\text{-Me(imid)}\})_2] \cdot (3 \cdot 0.5\text{C}_6\text{H}_5\text{Me})$ (Fig. 3) shows that the complex has a similar structural design to that of **2**, being composed of a $[\text{Sb}_3(\mu\text{-NCy})_3(\mu_3\text{-NCy})(2\text{-S}\{1\text{-Me(imid)}\})_2]^-$ anion which co-ordinates a Li^+ cation. The majority of the Sb–N bonds in **3** fall over a narrow range [1.997(9)–2.212(9) Å]. However, two longer Sb–N bonds are found between the $\mu_3\text{-N}$ centre and the four-co-ordinate, 10e antimony centres [Sb(1)–N(4) 2.212(9), Sb(3)–N(4) 2.309(10) Å; *cf.* Sb(2)–N(4) 2.039(9) Å]. These correspond to the use of orbitals

at one of the axial positions of the pseudo-trigonal bipyramidal environments of Sb(1) and Sb(3). Although a similar pattern of Sb–N bond lengths is also found in the $[\text{Sb}_3(\mu\text{-N})_3(\mu_3\text{-N})]$ core of **2**,⁶ the Sb–N bonds between the five-co-ordinate antimony centres and the $\mu_3\text{-N}$ centre are far more symmetrical in this complex [*i.e.* 2.335(5) and 2.311(4) Å]. The asymmetry of the $\mu_3\text{-N}$ cap in **3** reflects the extent of bonding of the pendant 2-S{1-Me(imid)} groups at the second axial position of Sb(1) and of Sb(3); the relatively long Sb–S bonds to Sb(1) [Sb(1)–S(1) 2.823(3) Å; *cf.* Sb(3)–S(3) 2.656(4) Å] being compensated for by shorter (presumably stronger) bonding of this atom to the $\mu_3\text{-N}$ centre. The co-ordination of the $[\text{Sb}_3(\mu\text{-NCy})_3(\mu_3\text{-NCy})(2\text{-S}\{1\text{-Me(imid)}\})_2]^-$ anion to Li^+ in **3** is highly asymmetrical. The shortest interactions occur with the $\mu\text{-N}$ centre of the core which bridges the two four-co-ordinate antimony atoms [Li–N(3) 2.13(2) Å] and with the two available imidazole N centres [Li–N(11) 2.03(2) and Li–N(31) 2.02(2) Å]. The strength of the co-ordination of the pendant imidazole groups pulls the Li^+ cation off-centre of the open Sb_3N_3 face of the anion, in a similar way to the interaction of the $[\text{Sb}_3(\mu\text{-NCy})_3(\mu_3\text{-NCy})(\text{O}^t\text{Bu})_2]^-$ anion with the K^+ cation of **2**.

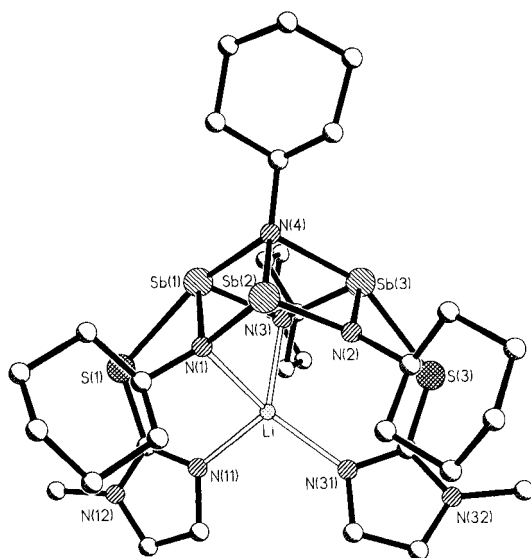


Fig. 3 Structure of molecules of $\text{Li}[\text{Sb}_3(\mu\text{-NCy})_3(\mu_3\text{-NCy})(2\text{-S}\{1\text{-Me(imid)}\})_2]$ **3** with H atoms omitted for clarity.

Table 2 Key bond lengths (Å) and angles (°) for $\text{Li}[\text{Sb}_3(\mu\text{-NCy})_3(\mu_3\text{-NCy})(2\text{-S}\{1\text{-Me(imid)}\})_2] \cdot 0.5\text{C}_6\text{H}_5\text{Me}$ **3**·0.5 $\text{C}_6\text{H}_5\text{Me}$

Sb(1)–N(1)	2.069(8)	Sb(3)–S(3)	2.656(4)
Sb(1)–N(3)	2.058(8)	Li–N(1)	2.40(2)
Sb(1)–N(4)	2.212(9)	Li–N(3)	2.13(2)
Sb(1)–S(1)	2.823(3)	Li–N(11)	2.03(2)
Sb(2)–N(1)	2.055(9)	Li–N(31)	2.02(2)
Sb(2)–N(2)	1.997(9)	C(1,3)–S(1,3)	mean 1.729
Sb(2)–N(4)	2.039(9)		
Sb(3)–N(2)	2.068(8)		
Sb(3)–N(3)	2.098(8)	Sb(3)···S(3a)	3.859(9)
Sb(3)–N(4)	2.309(10)	Sb(2)···Sb(2a)	4.16
N(1)–Sb(1)–N(3)	89.8(3)	N(2)–Sb(3)–S(3)	91.5(3)
N(1)–Sb(1)–N(4)	76.4(3)	N(3)–Sb(3)–S(3)	88.5(2)
N(3)–Sb(1)–N(4)	79.5(4)	N(4)–Sb(3)–S(3)	156.8(2)
N(3)–Sb(2)–S(1)	95.2(2)	N(1)–Li–N(3)	79.9(8)
N(1)–Sb(1)–S(1)	89.0(2)	N(1)–Li–N(11)	99.3(9)
N(4)–Sb(1)–S(1)	164.4(2)	N(1)–Li–N(31)	135(1)
N(1)–Sb(2)–N(2)	95.7(4)	N(3)–Li–N(11)	119(1)
N(1)–Sb(2)–N(4)	80.6(3)	N(3)–Li–N(31)	116(1)
N(2)–Sb(2)–N(4)	82.3(4)	N(11)–Li–N(31)	106(1)
N(2)–Sb(3)–N(3)	100.8(3)	Sb–μ–N(1,2,3)–Sb	103.4(5)–107.9(4)
N(2)–Sb(3)–N(4)	74.5(3)	Sb–μ ₃ –N(4)–Sb	96.0(4)–99.1(3)
N(3)–Sb(3)–N(4)	76.5(3)	Sb(3)–S(3)···Sb(3b)	83.0(4)
		S(3b)–Sb(3)···S(3)	97.0(4)

As a result, only one of the remaining $\mu\text{-N}$ centres of the anion interacts, weakly, with the Li^+ cation [Li–N(1) 2.40(2)], with the other being non-bonding [Li···N(2) 3.08(2) Å].

Two molecules of compound **3** associate into centrosymmetric, $\text{Sb}(\mu\text{-S})_2\text{Sb}$ -bridged dimers as a result of the interaction of one of the sulfur centres in each with a symmetry-related antimony centre of a neighbouring molecule (Fig. 4). The two symmetry related interactions [Sb(3b)···S(3a) 3.859(9) Å] in the $\text{Sb}(\mu\text{-S})_2\text{Sb}$ bridges of these dimers are within the sum of the van der Waals radii of Sb and S (*ca.* 4.05¹⁴), and similar to those involved in the association of molecules of $[\text{Sb}\{\text{S}(4\text{-MeC}_6\text{H}_4)\}_3]$ into a polymer in the solid state [3.773(8) Å].¹⁵ Further association of the dimers into polymeric (zigzag) chains results from weak Sb···Sb interactions. The separation involved [Sb(2)···Sb(2a) *ca.* 4.16 Å] is well within the value anticipated for a van der Waals interaction (*ca.* 4.40 Å¹⁴). The association of **3** into loosely linked dimers provides (at least at first sight) one possible reason for the presence of significantly different lengths of the Sb(1)–S(1) and Sb(3)–S(3) bonds within the molecule, and for the resulting distortion of the $[\text{Sb}_3\text{-}$

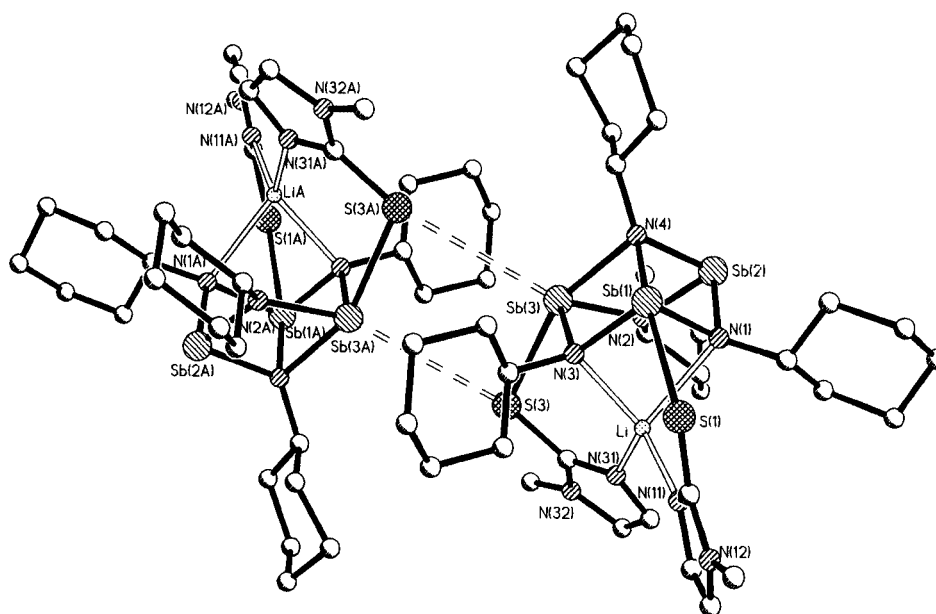


Fig. 4 Association of molecules of compound **3** into a loosely linked polymer structure by Sb···S and Sb···Sb interactions.

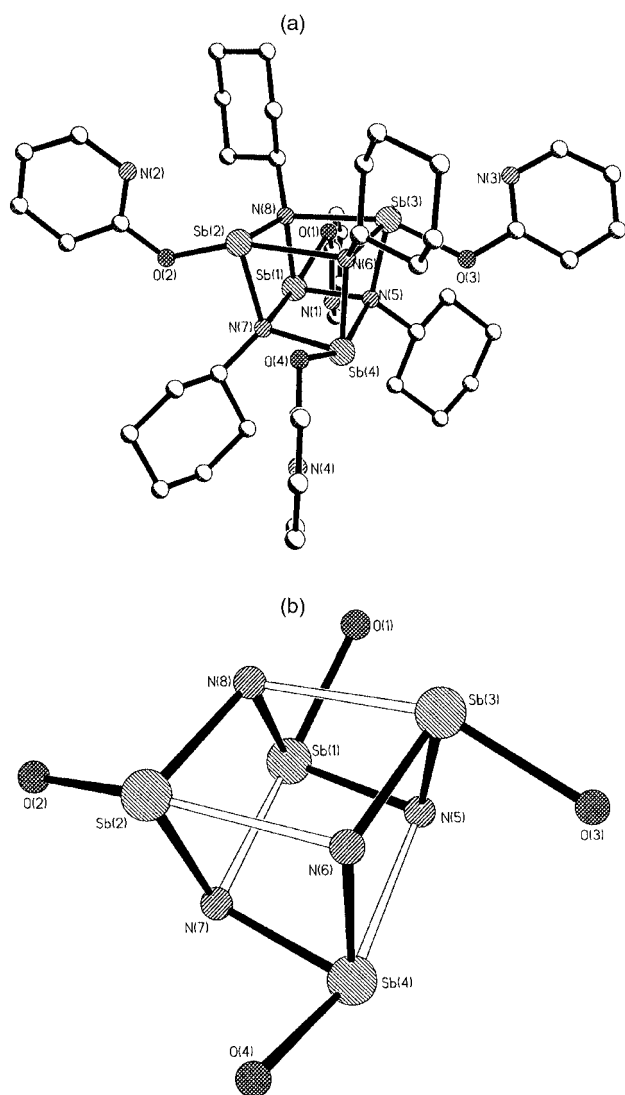


Fig. 5 (a) Structure of molecules of $[(2\text{-NC}_5\text{H}_4\text{O})\text{Sb}(\mu_3\text{-NCy})]_4$ **4** with H atoms omitted for clarity. (b) The core of **4** depicted as a folded Sb_4N_4 ring.

$(\mu\text{-N})_3(\mu_3\text{-N})$ core (discussed above). However, the observed shortening of the Sb(3)–S(3) bond [by *ca.* 0.17 Å relative to Sb(1)–S(1)] does not support this view since the increase in the co-ordination number of Sb(3) and the involvement of S(3) in the Sb–S···Sb bridge should result in an *increase* in the Sb–S bond length. It therefore appears more likely that the distortions within molecules of **3** stem primarily from the reorganisation of the core required for the donor imidazole nitrogen centres to engage the Li^+ cation. Some indication of this is provided by the very different orientations of the imidazole groups which co-ordinate the Li^+ cation. Whereas the imidazole ligand attached to S(1) is orientated with its plane roughly perpendicular to the Sb(1)Sb(2)Sb(3) plane of the anion (*i.e.* 92.9°), the imidazole group attached to S(3) adopts a less strained (tilted) orientation (with the plane of the imidazole ring being inclined at 50° with respect to the Sb_3 plane).

The low-temperature X-ray study of $[(2\text{-NC}_5\text{H}_4\text{O})\text{Sb}(\mu_3\text{-NCy})]_4 \cdot 0.5\text{C}_6\text{H}_5\text{Me}$ **4**·0.5 $\text{C}_6\text{H}_5\text{Me}$ reveals that the complex has a cubane structure in the solid state (Fig. 5a). In addition, there is half a molecule of toluene in the lattice. A search of the Cambridge Crystallography Data Base shows that very few discrete cubanes have structurally been characterised containing Sb_4X_4 cores (X = N, P, O, S or halogens). This structural motif is adopted in a few antimony(III) halide complexes, such as the anion $[\text{Cl}_3\text{Sb}(\mu_3\text{-Cl})]_4^{4-}$ ¹⁶ and the heterometallic $[\text{Cl}_3\text{Sb}(\mu_3\text{-Cl})\{\text{Fe}(\text{CO})_2\text{Cp}\}]$ (Cp = C_5H_5).¹⁷ In addition,

Table 3 Key bond lengths (Å) and angles (°) for $[(2\text{-NC}_5\text{H}_4\text{O})\text{Sb}(\mu_3\text{-NCy})]_4 \cdot 0.5\text{C}_6\text{H}_5\text{Me}$ **4**·0.5 $\text{C}_6\text{H}_5\text{Me}$

Sb(1)–N(5)	2.080(6)	Sb(3)–N(6)	2.082(6)
Sb(1)–N(7)	2.479(6)	Sb(3)–N(8)	2.292(6)
Sb(1)–N(8)	2.095(6)	Sb(4)–N(5)	2.543(6)
Sb(2)–N(6)	2.527(6)	Sb(4)–N(6)	2.075(6)
Sb(2)–N(7)	2.089(6)	Sb(4)–N(7)	2.080(6)
Sb(2)–N(8)	2.077(6)	Sb–O range	2.078(5)–2.101(5)
Sb(3)–N(5)	2.087(6)		
<hr/>			
N(5)–Sb(1)–N(7)	77.1(2)	N(5)–Sb(3)–N(8)	74.4(2)
N(8)–Sb(1)–N(7)	74.1(2)	N(6)–Sb(3)–N(8)	77.5(2)
N(5)–Sb(1)–N(8)	83.8(2)	N(5)–Sb(3)–N(6)	84.1(2)
O(1)–Sb(1)–N(7)	156.5(2)	O(3)–Sb(3)–N(8)	156.7(2)
O(1)–Sb(1)–N(5)	91.9(2)	O(3)–Sb(3)–N(5)	85.9(2)
O(1)–Sb(1)–N(8)	84.1(2)	O(3)–Sb(3)–N(6)	88.6(2)
N(7)–Sb(2)–N(6)	73.6(2)	N(6)–Sb(4)–N(5)	73.6(2)
N(8)–Sb(2)–N(6)	76.8(2)	N(7)–Sb(4)–N(5)	75.7(2)
N(8)–Sb(2)–N(7)	83.5(2)	N(6)–Sb(4)–N(7)	84.3(2)
O(2)–Sb(2)–N(6)	155.2(2)	O(4)–Sb(4)–N(5)	154.9(2)
O(2)–Sb(2)–N(7)	83.6(2)	O(4)–Sb(4)–N(6)	83.7(2)
O(2)–Sb(2)–N(8)	91.2(2)	O(4)–Sb(4)–N(7)	91.7(2)

cubane arrangements are observed for the imido/nitrido antimony(III) complex $[\{\text{ClSb}(\mu_3\text{-NSiMe}_3)\}_2\{\text{Sb}(\mu_3\text{-NSbCl}_2)\} - \{\text{ClSb}(\mu_3\text{-NSbCl}_3)\}]$ ¹⁸ and the imido antimony(V) complex $[\text{Cl}_3\text{Sb}(\mu_3\text{-NMe})]_4$.¹⁹ However, no simple imido antimony(III) complexes directly comparable to **4** have been structurally elucidated.

The association of the $[(2\text{-NC}_5\text{H}_4\text{O})\text{Sb}(\mu\text{-NCy})]_2$ dimer units of compound **4** into a cubane arrangement undoubtedly stems from the impact of the electronegative *exo*-O(2- $\text{C}_5\text{H}_4\text{N}$) ligands on the Lewis acidity of the antimony(III) centres. This situation can be compared to species of the type $[(\text{Me}_2\text{N})\text{Sb}(\mu\text{-NR})]_2$, which are all dimeric in the solid state as a result of the lower electronegativity of the Me_2N groups.⁹ The aggregation of the dimer units of **4** into a cubane structure has a direct analogue in antimony(V) imido complexes, $[\text{Ph}_3\text{Sb}(\mu\text{-NCH}_2\text{CH}_2\text{Ph})]_2$ being dimeric²⁰ whereas $[\text{Cl}_3\text{Sb}(\mu_3\text{-NMe})]_4$ adopts a cubane structure.¹⁹ Each of the antimony(III) centres of **4** adopts a similar, trigonal bipyramidal geometry in which an equatorial co-ordination site is occupied by a stereochemically active lone pair. The *exo*-O(2- $\text{C}_5\text{H}_4\text{N}$) ligands are located at an axial position within the co-ordination spheres of each Sb. This arrangement results in a large elongation of the Sb–N bonds within the core *trans* to the *exo*-O–Sb bonds (at the other axial position). The Sb–N bonds at the equatorial positions [range 2.075(6)–2.095(6) Å] are typical of those found in antimony(III) imido dimers,⁹ whereas those at the axial positions [range 2.479(6)–2.543(6) Å] are similar to Sb–N donor–acceptor interactions found in adducts of SbCl_3 .²¹ A similar diverse range of Sb–N bond lengths has been noted in the structure of the imido/nitrido antimony(III) complex $[\{\text{ClSb}(\mu_3\text{-NSiMe}_3)\}_2 - \{\text{Sb}(\mu_3\text{-NSbCl}_2)\}\{\text{ClSb}(\mu_3\text{-NSbCl}_3)\}]$.¹⁸ However, in this case the underlying pattern of Sb–N bond lengths within the Sb_4N_4 core (which is clearly identifiable in **4**) is complicated by the presence of different substituents bonded to the Sb and N. The pattern of Sb–N bond lengths in **4** prompts an alternative description of the structure as a folded, ‘tunnel-shaped’ Sb_4N_4 ring (shown in Fig. 5b).

Conclusion and closing remarks

The formation of the parent spiro frameworks in $\text{Li}\{(\text{Me}_2\text{N})\text{-Sb}(\mu\text{-NCy})_2\}_2\text{Sb}$ **1**·Li and $\text{Na}\{(\text{Me}_2\text{N})\text{Sb}(\mu\text{-NCy})_2\}_2\text{Sb}$ **1**·Na from the reactions of $^i\text{Pr}_2\text{NM}$ (M = Li or Na), CyNH_2 and $\text{Sb}(\text{NMe}_2)_3$ suggests that equilibration of the dimer $[(\text{Me}_2\text{N})\text{-Sb}(\mu\text{-NCy})]_2$ and the dianion $[\text{Sb}_2(\text{NCy})_4]^{2-}$ is involved in their formation (as outlined in Scheme 2). This equilibrium is also implicated in the reaction of **1**·Li with 2- $\text{NC}_5\text{H}_4\text{OH}$, producing the unusual cubane structure $[(2\text{-NC}_5\text{H}_4\text{O})\text{Sb}(\mu_3\text{-NCy})]_4$ **4**

[which is accessible by direct reaction of $[(\text{Me}_2\text{N})\text{Sb}(\mu\text{-NCy})_2]$ with $2\text{-NC}_5\text{H}_4\text{OH}$]. Overall, the reaction characteristics of the spiro- $[(\text{Me}_2\text{N})\text{Sb}(\mu\text{-NCy})_2]\text{Sb}^-$ anion **1** appear highly complicated. Whether selective reaction of the terminal Me_2N groups of this framework occurs or whether more extensive fragmentation arises probably depends largely on the acidity of the organic acid used. However, further influences such as the steric demands of the organic groups present and the presence of donor functionality within them may also play an important role. These additional influences, along with the electronegativity of the organic groups and the optimum co-ordination of the alkali metal cation, also play their part in the rearrangement of the spiro monoanion **1** to the *nido* structures of $[\text{K} \cdot \eta^6\text{-C}_6\text{H}_5\text{Me}][\text{Sb}_3(\mu\text{-NCy})_3(\mu_3\text{-NCy})(\text{O}^t\text{Bu})_2]$ **2** and $\text{Li}[\text{Sb}_3(\mu\text{-NCy})_3(\mu_3\text{-NCy})(2\text{-S}\{1\text{-Me(imid)}\})_2]$ **3**.

Experimental

General

Compounds **1**·Li, **1**·Na and **2–4** are air- and moisture-sensitive. They were handled on a vacuum line (in an efficient cupboard) using standard inert atmosphere techniques²² and under dry/oxygen-free argon. The compound $\text{Sb}(\text{NMe}_2)_3$ was prepared using the literature route, by transmetallation of SbCl_3 with LiNMe_2 (1:3 equiv),²³ purified by distillation and stored as a standardised solution in toluene; CyNH_2 and $^i\text{Pr}_2\text{NH}$ were distilled over CaH_2 and stored over molecular sieve prior to use and $2\text{-HS}\{1\text{-Me(imid)}\}$ and $2\text{-NC}_5\text{H}_4\text{OH}$ (Aldrich) were used as supplied. The thf , toluene, diethyl ether and hexane solvents were dried by distillation over sodium–benzophenone prior to the reactions. The products were isolated and characterised with the aid of an argon-filled glove-box fitted with a Belle Technology O_2 and H_2O internal recirculation system. Melting points were determined by using a conventional apparatus and sealing samples in capillaries under argon. The IR spectra were recorded as Nujol mulls using NaCl plates on a Perkin-Elmer Paragon 1000 FTIR spectrophotometer. Elemental analyses were performed by first sealing the samples under argon in air-tight aluminium boats (1–2 mg) and the contents of C, H and N analysed using an Exeter Analytical CE-440 Elemental Analyser. Proton NMR spectra were recorded on a Bruker WH 400 MHz spectrometer in dry deuteriated benzene (using the solvent resonances as the internal reference standard).

Details of the synthesis of compound **2** (which has been communicated previously) are given in reference 5.

Syntheses

1·Li. *n*-Butyllithium (12 ml, 18 mmol, 1.5 mol dm^{-3} in hexanes) was added to a solution of $^i\text{Pr}_2\text{NH}$ (2.55 ml, 18 mmol) in hexane (10 ml). After heating briefly to reflux, the solution of $^i\text{Pr}_2\text{NLi}$ was cooled to room temperature. This was added to a mixture of $\text{Sb}(\text{NMe}_2)_3$ (12.9 ml, 18 mmol, 1.4 mol dm^{-3} in toluene) and CyNH_2 (2.07 ml, 18 mmol) which had previously been brought briefly to reflux and cooled to room temperature. The resulting dark green reaction mixture was filtered and the filtrate reduced under vacuum until a yellow precipitate appeared. This was warmed back into solution. Storage at 25°C (24 h) gave a highly crystalline batch of **1**·Li. Typical yield 4.50 g, 88%. The identity of the complex was confirmed by obtaining the ^1H NMR spectrum and melting point, these being identical to those previously reported. The unit cell parameters of a crystal obtained by this route were also identical with those reported.⁶

1·Na. Diisopropylamine (2.8 ml, 20 mmol) was added to a suspension of PhCH_2Na (2.3 g, 20 mmol) in hexane (20 ml)–toluene (10 ml). After heating briefly to reflux, a mixture of $\text{Sb}(\text{NMe}_2)_3$ (14.3 ml, 20 mmol, 1.4 mol dm^{-3} in toluene) and

CyNH_2 (2.3 ml, 20 mmol) (prepared in a similar way to that used in the synthesis of **1**·Li) was added at room temperature. The resulting dark red reaction mixture was filtered and the filtrate reduced under vacuum until a yellow precipitate appeared. This was warmed back into solution. Storage at 25°C (24 h) gave a highly crystalline batch of **1**·Na. Yield 0.43 g, 7.5%. mp 196°C . ^1H NMR (d_6 -benzene, 250 MHz, $+25^\circ\text{C}$): δ 2.60 (s, 12 H, Me_2N) and *ca.* 2.5–1.0 (overlapping multiplets, 44 H, Cy). Found: C 38.9, H 6.6, N 9.7. Calc.: C 36.3, H 5.8, N 7.8%.

3. 1-Methyl-2-sulfanylimidazole (0.228 g, 2.0 mmol) was added to a solution of compound **1**·Li (0.85 g, 2.0 mmol) in toluene (20 ml) at 25°C . An immediate reaction occurred with the formation of a colourless precipitate. This was dissolved by heating gently. Storage at room temperature gave yellow cubes of **3**· $0.5\text{C}_6\text{H}_5\text{Me}$. Yield 0.18 g, 18%. Decomp. 225°C to brown solid. ^1H NMR (d_6 -benzene, 250 MHz, $+25^\circ\text{C}$): δ = 7.20 (d, aromatic protons of $2\text{-S}\{1\text{-Me(imid)}\}$), 6.40 [d, 2 H, aromatic protons of $2\text{-S}\{1\text{-Me(imid)}\}$], 7.15 (m, *ca.* 2.5 H, C_6H_5 of toluene), 3.20 (s, 6 H, Me), 2.70–0.70 (overlapping multiplets, 44 H, Cy) and 2.15 (s, *ca.* 1.5 H, Me of toluene). Found: C 40.2, H 5.2, N 10.5. Calc. for **3**· $0.5\text{C}_6\text{H}_5\text{Me}$: C 41.2, H 5.6, N 10.8%.

4. *Method A*. 2-Hydroxypyridine (0.076 g, 0.71 mmol) was added to a solution of compound **1**·Li (0.30, 0.35 mmol) in toluene (20 ml) at 25°C . The solution developed a green tinge and became slightly cloudy. The reaction mixture was brought to reflux briefly. The solid produced was partially dissolved by the addition of thf (5 ml) and heating. Filtration produced a lemon-yellow solution. The solvent was removed under vacuum until precipitation commenced, this being heated back into solution. Storage at -15°C (2 weeks) produced a crop of small white crystals of **4**· $0.5\text{C}_6\text{H}_5\text{Me}$. Yield 0.034 g, 10%.

Method B. A solution of the dimer $[(\text{Me}_2\text{N})\text{Sb}(\mu\text{-NCy})_2]$ was prepared *in situ* by the reaction of CyNH_2 (0.69 ml, 6.0 mmol) with $\text{Sb}(\text{NMe}_2)_3$ (3.05 ml, 1.97 mol dm^{-3} solution in toluene, 6.0 mmol) in toluene (20 ml). Solid 2-hydroxypyridine was added (0.571 g, 6.0 mmol). The mixture was brought to reflux. A precipitate formed was filtered off and the lemon-yellow filtrate reduced until precipitation commenced. The precipitate was heated back into solution and storage at 25°C (12 h) gave large cubic crystals of **4**· $0.5\text{C}_6\text{H}_5\text{Me}$. Yield 0.598 g (31%). Mp 190°C . ^1H NMR (d_6 -benzene, 250 MHz, $+25^\circ\text{C}$): δ 8.21 (m, 4 H), 7.25 (m, 4 H), 7.15 (m, 2.5 H, C_6H_5 of toluene), 6.75 (apparent d, 1 H), 6.51 (mult, 1 H), 2.45–0.95 (overlapping sharp multiplets, 44 H, Cy) and 2.22 (s, 1.5 H, Me of toluene). Found: C 43.7, H 5.0, N 8.6. Calc. for **4**· $0.5\text{C}_6\text{H}_5\text{Me}$: C 43.9, H 5.0, N 8.6%.

X-Ray crystallographic studies

Crystals of compounds **1**·Na, **3**· $0.5\text{C}_6\text{H}_5\text{Me}$ and **4**· $0.5\text{C}_6\text{H}_5\text{Me}$ were mounted directly from solution under argon using an inert oil which protects them from atmospheric oxygen and moisture.²⁴ X-Ray intensity data for **1**·Na were collected with a Stoe-Siemens AED diffractometer using a θ – ω scan mode, for **3**· $0.5\text{C}_6\text{H}_5\text{Me}$ with a Siemens P4 diffractometer using an ω – 2θ scan mode, and for **4**· $0.5\text{C}_6\text{H}_5\text{Me}$ on a Nonius Kappa 4 CCD diffractometer. For **1**·Na and **3**· $0.5\text{C}_6\text{H}_5\text{Me}$ a semi-empirical absorption correction based on ψ scans was applied. Details of the data collection, refinement and crystal data are listed in Table 4. A planar region of residual electron density in **4** was interpreted as a severely disordered half toluene molecule (in accordance with the analytical and spectroscopic data obtained on the complex). The half toluene molecule is disordered over an inversion centre.

CCDC reference number 186/1950.

See <http://www.rsc.org/suppdata/dt/b0/b001322f/> for crystallographic files in .cif format.

Table 4 Crystal data for Na[$\{(\text{Me}_2\text{N})\text{Sb}(\mu\text{-NCy})_2\}_2\text{Sb}\}$ **1**·Na, Li[Sb $_3(\mu\text{-NCy})_3(\mu_3\text{-NCy})(2\text{-S}\{1\text{-Me(imid)}\})_2\}$ **3**·0.5C $_6\text{H}_5\text{Me}$ and [(2-NC $_5\text{H}_4\text{O}$)Sb($\mu_3\text{-NCy}$)] $_4$ ·0.5C $_6\text{H}_5\text{Me}$ **4**·0.5C $_6\text{H}_5\text{Me}$

Formula	1 ·Na C $_{28}\text{H}_{56}\text{N}_6\text{NaSb}_3$	3 ·0.5C $_6\text{H}_5\text{Me}$ C $_{35.50}\text{H}_{58}\text{LiN}_8\text{S}_2\text{Sb}_3$	4 ·0.5C $_6\text{H}_5\text{Me}$ C $_{47.50}\text{H}_{66}\text{N}_8\text{O}_4\text{Sb}_4$
Formula weight	865.03	1033.21	1300.08
Crystal system	Monoclinic	Triclinic	Triclinic
Space group	$P2_1/c$	$P\bar{1}$	$P\bar{1}$
$a/\text{\AA}$	9.599(2)	11.177(3)	12.793(3)
$b/\text{\AA}$	21.379(4)	13.746(3)	14.864(3)
$c/\text{\AA}$	17.097(3)	15.173(4)	15.340(3)
α°	—	70.146(10)	65.45(3)
β°	99.82(3)	87.83(2)	74.73(3)
γ°	—	89.668(19)	80.35(3)
$U/\text{\AA}^3$	3457.2(11)	2191.0(9)	2554.0(9)
Z	4	2	2
μ/mm^{-1}	2.366	1.965	2.142
TK	180(2)	223(2)	180(2)
Reflections collected	6596	7104	20787
Independent reflections	4499	6004	8998
$R1, wR2[I > 2\sigma(I)]$	0.079, 0.199	0.062, 0.164	0.044, 0.132
(all data)	0.116, 0.226	0.105, 0.205	0.086, 0.132

Acknowledgements

We gratefully acknowledge the EPSRC (A. B., N. F., A. D. H., S. J. K., M. McP.), The Leverhulme Trust (M. A. B.) and Electron Tubes, Ltd., U.K. (A. D. H.) for financial support.

References

- M. A. Beswick and D. S. Wright, *Coord. Chem. Rev.*, 1998, **176**, 373, and references therein.
- (a) M. A. Beswick, C. A. Harmer, M. A. Paver, P. R. Raithby, A. Steiner and D. S. Wright, *Inorg. Chem.*, 1997, **36**, 1740; (b) D. Barr, A. J. Edwards, S. Pullen, M. A. Paver, M.-A. Rennie, P. R. Raithby and D. S. Wright, *Angew. Chem.*, 1994, **106**, 1960; *Angew. Chem., Int. Ed. Engl.*, 1994, **33**, 1875; (c) A. Bashall, M. A. Beswick, C. N. Harmer, M. A. Paver, M. McPartlin and D. S. Wright, *J. Chem. Soc., Dalton Trans.*, 1998, 517.
- A. Bashall, M. A. Beswick, E. A. Harron, A. D. Hopkins, S. J. Kidd, M. McPartlin, P. R. Raithby, A. Steiner and D. S. Wright, *Chem. Commun.*, 1999, 1145; A. Bashall, H. Ehlenberg, M. A. Beswick, S. J. Kidd, J. S. Palmer, P. R. Raithby, J. M. Rawson and D. S. Wright, unpublished results.
- M. A. Beswick, C. N. Harmer, A. D. Hopkins, M. McPartlin and D. S. Wright, *Science*, 1998, **281**, 1500.
- M. A. Beswick, N. Choi, A. D. Hopkins, M. McPartlin, M. A. Paver and D. S. Wright, *Chem. Commun.*, 1998, 261.
- A. J. Edwards, M. A. Paver, M.-A. Rennie, C. A. Russell, P. R. Raithby and D. S. Wright, *Angew. Chem.*, 1994, **106**, 1334; *Angew. Chem., Int. Ed. Engl.*, 1994, **33**, 1277.
- A. Bashall, M. A. Beswick, C. N. Harmer, A. D. Hopkins, M. McPartlin, M. A. Paver, P. R. Raithby and D. S. Wright, *J. Chem. Soc., Dalton Trans.*, 1998, 1389.
- M. A. Beswick, A. Bashall, A. D. Hopkins, S. J. Kidd, Y. G. Lawson, M. McPartlin, P. R. Raithby, A. Rothenberger, D. Stalke and D. S. Wright, *Chem. Commun.*, 1999, 739.
- For example, A. J. Edwards, M. A. Paver, M.-A. Rennie, C. A. Russell, P. R. Raithby and D. S. Wright, *J. Chem. Soc., Dalton Trans.*, 1994, 2963; M. A. Beswick, C. N. Harmer, A. D. Hopkins, M. A. Paver, P. R. Raithby and D. S. Wright, *Polyhedron*, 1998, **17**, 745.
- A. L. Allred, *J. Inorg. Nucl. Chem.*, 1961, **17**, 215.
- E. Block, G. Ofori-Okai, H. Kang, J. Wu and J. Zubieta, *Inorg. Chem.*, 1991, **30**, 4784.
- M. Veith and J. Böhnlein, *Chem. Ber.*, 1989, **122**, 603; M. Veith, A. Spaniol, J. Pohlmann, F. Gross and V. Huch, *Chem. Ber.*, 1996, **126**, 2625; M. Neimeyer and P. P. Power, *Organometallics*, 1996, **15**, 4105.
- M. Björgvinsson, H. W. Roesky, G. M. Sheldrick and F. Pauer, *Chem. Ber.*, 1992, **123**, 767.
- A. Bondi, *J. Phys. Chem.*, 1964, **68**, 441.
- W. Clegg, M. R. J. Elsegood, L. J. Farrugia, F. J. Lawlor, N. C. Norman and A. J. Scott, *J. Chem. Soc., Dalton Trans.*, 1995, 2129.
- U. Ensinger, W. Schwarz and A. Smidt, *Z. Naturforsch., Teil B*, 1982, **37**, 1584.
- Trinh-Toan and L. F. Dahl, *Inorg. Chem.*, 1976, **15**, 2953.
- M. Rhiel, F. Weller, J. Pebler and K. Dehnicke, *Angew. Chem.*, 1994, **106**, 599; *Angew. Chem., Int. Ed. Engl.*, 1994, **33**, 569.
- W. Neubert, H. Pritzkow and H. P. Latscha, *Angew. Chem.*, 1988, **100**, 298; *Angew. Chem., Int. Ed. Engl.*, 1988, **27**, 287.
- A. J. Edwards, M. A. Paver, P. Pearson, P. R. Raithby, M.-A. Rennie, C. A. Russell and D. S. Wright, *J. Organomet. Chem.*, 1995, **503**, C29.
- For example, R. Hulme, *J. Chem. Soc. A*, 1968, 2448.
- D. F. Shriver and M. A. Drezdon, *The Manipulation of Air-Sensitive Compounds*, 2nd edn., Wiley, New York, 1986.
- K. Moedritzer, *Inorg. Chem.*, 1964, **3**, 609; F. Ando, T. Hayashi, K. Ohashi and J. Kotetsu, *J. Nucl. Chem.*, 1991, **30**, 2011.
- T. Kottke and D. Stalke, *J. Appl. Crystallogr.*, 1993, **26**, 615.